Sound transmission through double-glazed window: numerical and experimental analyses

Chaima SOUSSI [1]; Mathieu AUCEJO[1]; Walid LARBI[1]; Jean-François DEÜ[1]

[1] Conservatoire national des arts et métiers, LMSSC, Paris, France

ABSTRACT

Double-glazing is widely used in constructions due of their sound insulation performance. According to the standards, the prediction of their acoustic performances is carried out in laboratory using two reverberant rooms. It's well known that, in the low frequency range below the Schroeder frequency, the presence of these rooms can affect the measurements due to their modal behavior. Thus, the prediction of their acoustic and vibratory behavior is very complicated and depends on several factors such as the used materials, the boundary conditions and the diffuseness of the acoustic field.

In this work, experimental and numerical studies on the vibroacoustic behavior in low frequency range of double-glazing are presented. First, a finite element model for the proposed fluid-structure coupled problem is proposed. Experimental modal analysis of the structure is then detailed. The results of this analysis are used to validate a numerical model of double-glazing. Finally, various models for numerical sound reduction prediction of double glazing are presented and compared.

Keywords: Double-glazing, Experimental modal analysis, Finite element.

1. INTRODUCTION

Double glazing is often used in noise reduction since a relatively high transmission loss is achieved by introducing of an acoustic gap between the panels. Due to various effects of fluid-structure interaction, the prediction of the acoustic performance of the double wall remains very complicated in the low frequencies whatever the method used. We propose in this paper a reliable method based on experimental measurements and numerical analyzes able to predict the vibroacoustic behavior of double-glazing. In the literature, the article (1), (2) and (3) studied experimentally the transmission loss through single, double and triple glazing. In (4), the effect of boundary conditions on this acoustic indicator of double panels was investigated. A comparison of different type of glass models can be found in (5). For the numerical prediction approaches, several methods are available. The choice of the numerical method depends on the computational cost and the treated frequency band. The Finite Element Method (FEM) is suitable to treat problems in low frequencies. In (6), this method is applied to develop a model of a sandwich plate with viscoelastic core. The FEM is applied in (7) by the authors for the different layers of the sound barrier coupled to a variational Boundary Element Method (BEM) to account for fluid loading.

The present paper is organized as follows: In the first part, a finite element formulation of the vibro-acoustic problem is presented. The second section is devoted to the modal experimental analysis of the double-glazing. The impact hammer test is used to evaluate the modal parameters (natural frequencies, mode shape and damping) which were used to recalibrate a numerical model of the studied system. In the last part, numerical evaluation of the acoustic performances of double-glazing is presented. The difficulties of the numerical models are related to the representation of (i) the acoustic excitation and (ii) the effects of the emitting and receiving rooms. Thus, four configurations are proposed from which two are selected. We study the difference between the case where an acoustic room is modeled and where the Rayleigh integral is used. The effect of the damping and the acoustic impedance is also analyzed.

2. Finite element formulation for the vibro-acoustic problem

Let us consider the linear vibrations of an elastic structure filled with a homogeneous, inviscid and compressible fluid, neglecting gravity effects. This configuration is chosen to model the double-glazing system. We establish in this section the local equations of the coupled problem and the

[1] Chaima.soussi@lecnam.net

corresponding finite element matrix equations.

2.1 Local equations of the problem

We consider an elastic structure occupying the domain Ω_{S^i} (i=1, 2) at the equilibrium. The structure is subjected to a prescribed displacement $\mathbf{u}$ on a part Γ_u and to surface force density $\mathbf{F}^d$ on the complementary part of its external boundary. The interior fluid domain is denoted by Ω_F and the fluid–structure interface by Σ (see Figure 1).

We note $\boldsymbol{\sigma}$, the stress tensor and ρ_s, the density of the structure. In addition, since the compressible fluid is assumed to be inviscid, instead of describing its motion by a fluid displacement vector field, which requires an appropriate discretization of the fluid irrotationality constraint, we use the pressure scalar field p. Let us note k the wave number in the fluid ($k = \omega/c_F$) where c_F is the speed of wave propagation in the fluid, ρ_F the mass density of the fluid, and $\mathbf{n}^s$ the normal of the structure. The local equations of the fluid-structure coupled problem described previously are:

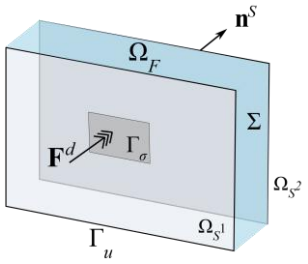


Figure 1 – Double-glazing system

$$
\begin{cases}
\mathrm{div}\boldsymbol{\sigma}(\mathbf{u}) + \rho_s\omega^2\mathbf{u} = 0 & \text{in } \Omega_{S^i} \quad (1)\\
\boldsymbol{\sigma}(\mathbf{u})\mathbf{n}^s = \mathbf{F}^d & \text{on } \Gamma_\sigma \quad (2)\\
\mathbf{u} = \mathbf{u}^d & \text{on } \Gamma_u \quad (3)\\
\boldsymbol{\sigma}(\mathbf{u})\mathbf{n}^s = p\mathbf{n}^F & \text{on } \Sigma \quad (4)\\
\Delta p + k^2 p = 0 & \text{in } \Omega_F \quad (5)\\
\nabla p.\mathbf{n}^F = \rho_F\omega^2\mathbf{u}.\mathbf{n} & \text{on } \Sigma \quad (6)
\end{cases}
$$

Eq. (1) corresponds to the elasto-dynamic equation in absence of body force; Eqs. (2), (3) are the prescribed mechanical boundary conditions represent the surface forces applied on Γ_σ and the displacement imposed on Γ_u ,respectively; Eq. (4) results from the action of pressure forces exerted by the fluid on the structure; Eq. (5) is the Helmholtz equation; and Eq. (6) is the kinematic interface fluid–structure condition on Σ.

2.2 Finite element discretization

In the finite element context, the previous vibro-acoustic problem is described in terms of structure displacement u and acoustic pressure p. The discretization of the variational formulation associated to the previous equations (1) to (6) leads to the following matrix system (see (6) for details):

$$
\left(\begin{bmatrix} \mathbf{K}_u & -\mathbf{C} \\ 0 & \mathbf{K}_\mathrm{p} \end{bmatrix} + i\omega \begin{bmatrix} \mathbf{D}_u & 0 \\ 0 & \mathbf{D}_p \end{bmatrix} - \omega^2 \begin{bmatrix} \mathbf{M}_u & 0 \\ \mathbf{C}^\mathrm{T} & \mathbf{M}_p \end{bmatrix} \right) \begin{bmatrix} \mathbf{U} \\ \mathbf{P} \end{bmatrix} = \begin{bmatrix} \mathbf{F} \\ 0 \end{bmatrix} \quad (7)
$$

with $\mathbf{K}_u$, $\mathbf{M}_u$ and $\mathbf{D}_u$ are the structural stiffness, mass and damping matrices, $\mathbf{K}_\mathrm{p}$, $\mathbf{M}_p$ and $\mathbf{D}_p$ are the associated acoustic matrices, $\mathbf{C}$ is the fluid-structure coupling matrix and $\mathbf{F}$ is the structural load.

3. Experimental analysis of the double-glazing

The modal analysis of the structure is essential for understanding its dynamic performance. In this section, we are interested in experimental modal characterization (resonant frequencies and damping coefficients) of double glazing. The experimental results will be used for the validation of a developed numerical model.

3.1 Description of the structure

The complete structure presented in Figure 2.a is a domestic wooden window with two symmetrical opening mounted on a frame. The model is 1.45 m wide by 1.5 m high. It weights approximately 76 kg. Each opening is composed of double-glazed surrounded by a rubber seal and incorporated in a sash which is composed of two stiles and two rails (Figure 2.b). The complete, the window is composed of 92 pieces of different sizes and different materials such are wood, glass, rubber, etc.

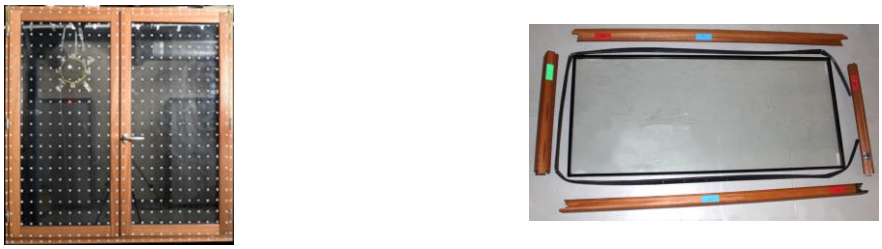


Figure 2 – (a) Wooden window, (b) Components of one opening

The double-glazing, presented in Figure 3, combines two glass panes separated by a 18 mm spacer and an argon gap. It is 0.581 m wide by 1.309 m high. The polyamide spacer is filled at least half by the desiccant, which is a silicon material used to absorb the moisture within the cavity through the perforations of the spacer. The gluing of the spacer on the window is done with a butyl type sealant or resistant silicone. All the parts are connected and sealed with a visible silicone located around the outside edge.

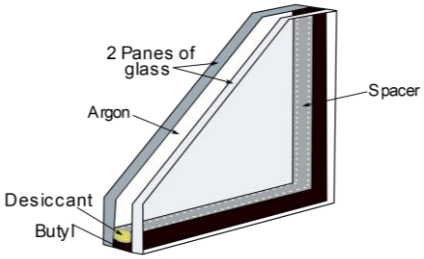


Figure 3 – Details of the double-glazing

3.2 Experimental Modal Analysis

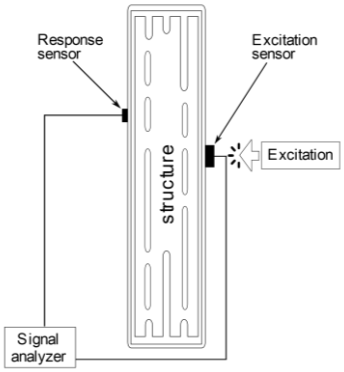
The Experimental Modal Analysis (EMA) is a tool to characterize the modal properties of a complex structure through the identification of its natural frequencies, mode shapes and modal damping ratios. Basically, the implementation of an EMA requires the measurement of the Frequency Response Function (FRF) of the considered structure at different points of the latter (Figure 4). In this work, the "roving hamme" test is used with an impact hammer and three reference accelerometers. This method consists in fixing accelerometers and then impact the structure at several points.

3.3 Impact testing considerations

The basic principle of the roving hammer test is to hit the structure with an impulse and then measure its response. This needs to be done at several points on the structure to obtain a fair representation of the mode shapes. The impact hammer is equipped with a force sensor and a nylon tip.



Accelerometer





Impact hammer

Figure 4 – The device of modal analysis

The suspended double-glazing (see Figure 5) is meshed into 153 nodes. Excitation is done in all nodes with an average of three impacts and measurements are performed up to 400 Hz, with 0.5 Hz frequency resolution.

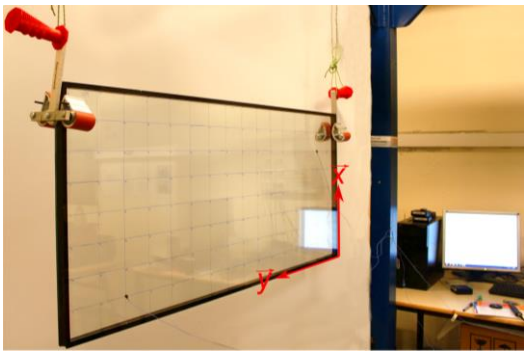


Figure 5 – Suspended double-glazing

3.4 Numerical Model

In this section, the double glazing experimentally tested is modeled numerically with the finite element method. The objective is to find a numerical representation of the structure able of reproducing its dynamic modal behavior. Thus, the model found will be used for acoustic studies.

The numerical model consists of two 2D shells representing the two glass panels separated by a three-dimensional cavity filled with argon (sound speed 317 m/s and density 1.6 kg/m^3). The structure is considered free in the space. The properties of the glass defined for the two planes are $E = 60$ GPa; $\rho = 2450$ (kg/m^3) and ν =0.23. An equivalent material, whose properties are $E = 0.1$ GPa ; $\rho = 1000$ (kg/m^3) and ν=0.49, is defined for the group «spacer + butyl + desiccant». Quadrilateral shell elements for the solid and hexahedral elements for the fluid are used for the finite element discretization. The mesh sizes for the structure and the acoustic domain are controlled by the wavelength λ (m) which depends on the frequency range of interest. For the acoustic domain, the acoustic wavelength is $\lambda_a = c/f$ where c (m/s) is the speed of sound. For the structure, the flexural wavelength is $\lambda_f = \sqrt{2\pi/f}\,(D/M)^{1/4}$ where D (Pa.m^3) is the flexural rigidity and M(kg/m²) the surface mass density. Since it is recommended to use 6 elements per wavelength, we obtain a model containing 35604 degrees of freedom.

3.5 Results and discussion

Firstly, in order to validate the experimental measurements, the principle of reciprocity must be verified. It means that the frequency response function measured between two points must be the same regardless of which of them is input or output. Two cases are tested; the first one where the excitation point P1 and the measurement P2 are in the same glass pane. The second one where the excitation point is in the first glass pane and the measurement point is in the second one. The results presented in Figure 6 show that the reciprocity is insured since the curves are superposed following the permutation between the excitation and measurement points.

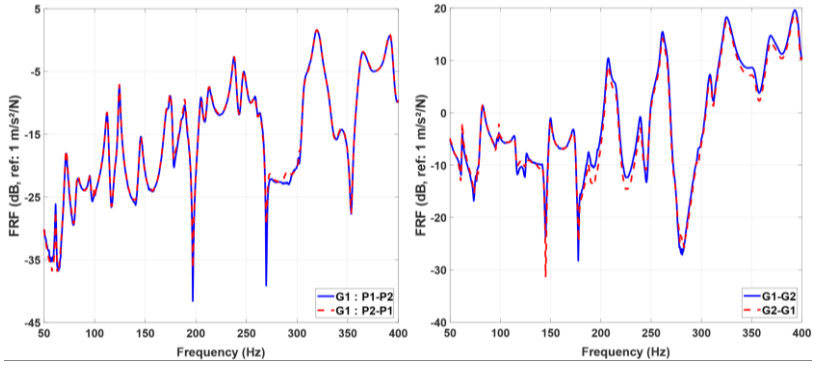


Figure 6 – Verification of the reciprocity

For analyzing the experimental data, a home-made EMA toolbox based on the pLSCF (polyreference Least Squares Complex Frequency domain) (8) has been implemented. Figure 7 shows the comparison of the first ten natural frequencies of the structure obtained from the experimental and numerical analysis. For a such complex structure, results are considered satisfying since the maximum difference of natural frequency is 6.8 %, observed for Mode 8.

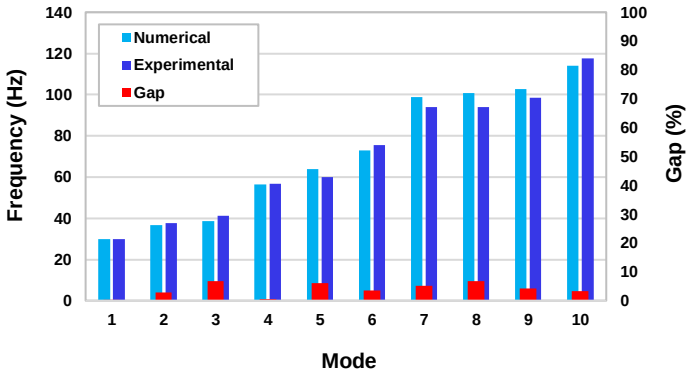
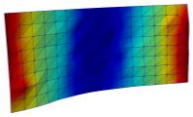
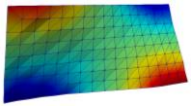
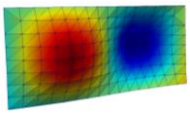
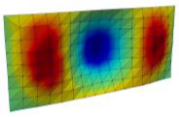
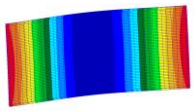
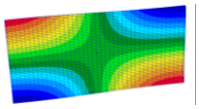
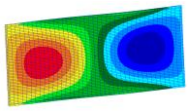
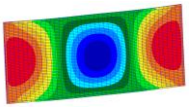


Figure 7 – Comparison of the first ten experimental and numerical eigenfrequencies of the double-glazing

Table 1 presents a comparison of modes shapes 1, 2 3 and 6 experimentally measured and found by finite element method. Once again, a good agreement between the two methods is observed.

Table 1–Comparison of experimental and numerical mode shapes

Mode	1	2	3	6
Experimental				
	29.9 Hz	37.7 Hz	41.2 Hz	75.5 Hz
Numerical				
	29.8 Hz	36.6 Hz	38.6 Hz	73 Hz

The modal damping is often the parameter extracted with the greatest uncertainty (9). Results of the first ten modal damping presented in the Figure 8 show that this parameter variates from 0.9 % at the 6th mode to reaches the maximum at the 2nd mode with a value of 11.3 %. These data will be used for vibroacoustic numerical simulations of the problem.

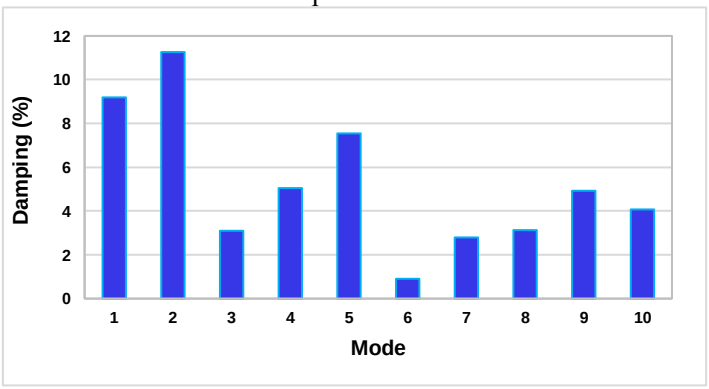


Figure 8 – Experimental modal damping of the double-glazing

4. Measurements of sound transmission

4.1 Experimental set-up

The airborne sound insulation of building elements such as walls, doors, windows can be evaluated in laboratory according to standards norms (10). These standards allow the determination of the acoustic performances of the structures by the measurement of the sound reduction index. Measurement takes into consideration two adjacent reverberation rooms, separated by a common wall containing an opening in which the test element is mounted (see Figure 9). During the laboratory measurements, R is defined as the difference between the average sound pressure levels in the source

room and in the receiving room with a correction term considering the acoustic absorption A (m²) and the area of the test specimen S (m²):

$$R = L_s - L_r + 10\log_{10}(S/A) \quad (8)$$

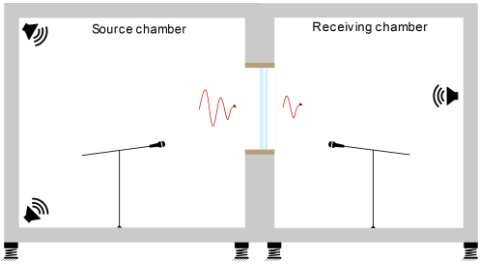


Figure 9 – Experimental set-up of acoustic experimental test

4.2 Other configurations

Standards (10) assume that acoustic excitation is a diffuse field for the entire frequency band of measurement [100 Hz - 5000 Hz]. This condition is respected only beyond the "Schroeder frequency" of the room which marks the limit between the modal behavior and the diffuse field. This frequency is generally high and inversely proportional to the dimensions of the chamber.

At low frequencies, to treat the problem numerically by respecting the condition of the diffuse field, it is necessary to model a room whose dimensions are larger than the wavelength which is penalizing for the cost of computation. To overcome this problem, the plane wave superposition method is an effective solution. The technique consists in exciting the structure by a diffuse sound field (Figure 10.b). This solution therefore makes it possible to avoid modeling the emitting chamber. On the reception side, it can be assumed that the window radiates in a semi-infinite field without considering the receiving acoustic cavity (Figure 10.c). The combination of these two solutions, presented by the last configuration (Figure 10.d), makes it possible to reduce the size of the model and to avoid the modal effects of the rooms.

For numerical methods, the FEM method is used to model the window. For the modeling of the transmission and reception sides, the method used will depend on the chosen configuration. For example, for cases where both chambers are modeled, the FEM will be used since it is a bounded problem. For the cases of radiation in a free field corresponding to an unbounded problem, several solutions are presented (Rayleigh, BEM or also FEM combined with a perfectly matched layer (PML) for the far field.

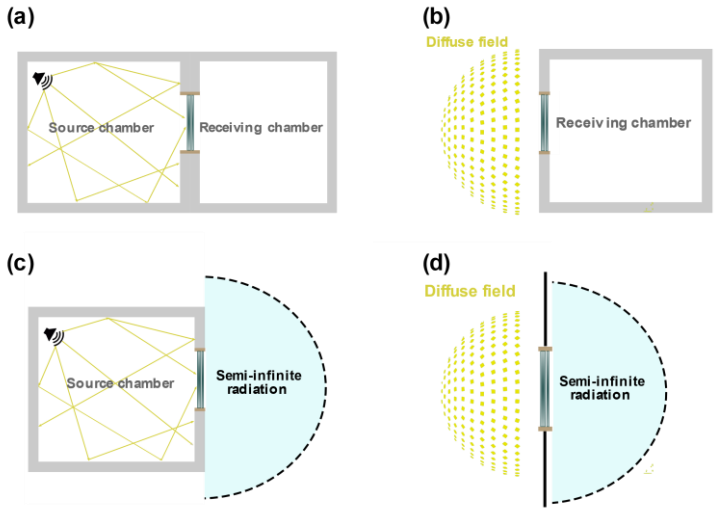


Figure 10 – Different configurations considered for problem resolution

4.3 Numerical analysis

In this section, we focus our attention on the numerical analysis of configurations (b) and (d) to calculate the sound transmission of the double-glazing model previously established. For the two cases considered, the excitation of the structure is a diffuse sound field which is a superposition of random

plane waves in phase and direction making a uniform sound pressure at every point. The difference between the two analyses is the modelling of the receiving side: In the first configuration, the structure radiates in a 3.25×4×5 m^3 rigid rectangular cavity. The structure is clamped to a wall of the room. In the second case, the Rayleigh integral is used in the receiving side. This condition represents the acoustic radiation of a plane structure mounted in a rigid baffle in a half-space. Since direct frequency analyses are carried out, only materials damping is defined in the models.

4.3.2 Results and discussion

The carried numerical models allow to determinate the Transmission Loss of the structure (TL). This parameter is calculated in decibels (dB) as the ratio of the sound power incident w_i by the sound power transmitted w_t by the structure:

$$\mathrm{TL} = 10\log_{10}(w_i/w_t) \tag{9}$$

A comparison of the results in narrow band and 1/3 octave is established. The frequency range for narrow band figure goes from 1Hz to 600 Hz and from 31 Hz to 500 Hz for the 1/3 octave band presentation. A damping of 1% is used for all the material of the models. Firstly, a comparison of the TL calculated with the two configurations (b) and (d) is illustrated in the Figure 11. We can see in the narrow frequency band, a fluctuation of the TL at the low frequencies with the presence of the receiving room. This is explained by the modal behavior of the acoustic cavity. In fact, the coincidence of the excitation with the acoustic natural frequencies, for example Mode 2 at 43 Hz, Mode 7 at 68 Hz and Mode 28 at 132 Hz presented in Figure 11, causes an increase in the sound pressure level in the room, which leads to a decrease of the measured TL. This is not the case when the structure radiated in a semi-infinite domain. The sound reduction calculated in the two configurations becomes similar from 200 Hz, a value around the cutoff frequency of the acoustic cavity.

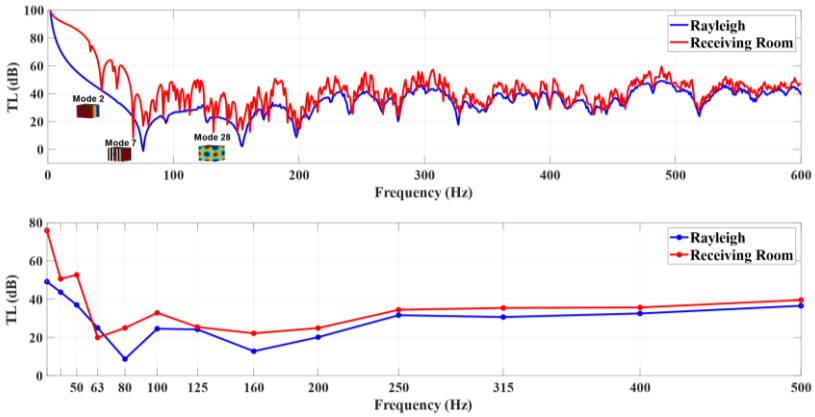


Figure 11 – Comparison of the TL between the two configurations in the narrow and 1/3 octave band

The second aim of this section is to study the influence of the damping in the TL of the structure. For this, three analyses are made with the configuration (d). Results presented by the Figure 12 disclosed the fact that the damping smooths the curve of the TL and influences considerably the results above 100 Hz. At 500 Hz, the model without damping present a results 15 dB lower than the case with 1% damping. Below 100 Hz, the TL of all models present a similar behavior.

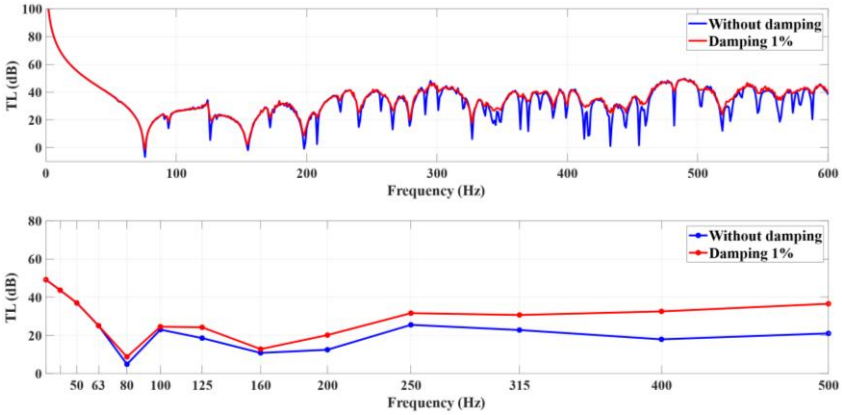


Figure 12 – Effect of the damping in the TL of the double-glazing (configuration d)

5. CONCLUSIONS AND PERSPECTIVES

In this work, the vibroacoustic behavior of the double-glazing glass is studied. First, the modal behavior of the structure is experimentally identified and validated with the finite element method. The established numerical model was used to carry out different acoustic analyses. The numerical examples show that the presence of the acoustic room has a significant influence on the TL in the very low frequencies due to its modal behavior below the Schneider frequency. In addition, the dynamic damping and the impedance don't have an influence below 100 Hz but improve the acoustic performances in the higher frequencies.

Within this framework, many future investigations and developments can be considered among which: the calculation of the TL with other configurations to study the influence of the acoustic cavities and their geometries; the influence of the structural and the acoustic boundary conditions; the recalibration of a model of one opening and then the hole window.

ACKNOWLEDGEMENTS

The authors would like to express their thanks to CODIFAB (Comité professionnel de développement des industries françaises de l'ameublement et du bois) for its financial support.

REFERENCES

1. Quirt JD. Sound transmission through windows I. Single and double glazing. J Acoust Soc Am. 1982 Sep;72(3): p. 834–44.
2. Quirt JD. Sound transmission through windows II. Double and triple glazing. J Acoust Soc Am. 1983 Aug;74(2): p. 534–42.
3. Tadeu AJB, Mateus DMR. Sound transmission through single, double and triple glazing. Experimental evaluation. Appl Acoust. 2001 Mar;62(3): p. 307–25.
4. Xin FX, Lu TJ. Analytical modeling of sound transmission through clamped triple-panel partition separated by enclosed air cavities. Eur J Mech - A Solids. 2011 Nov 1;30(6): p. 770–82.
5. Miskinis K, Dikavicius V, Bliudzius R, Banionis K. Comparison of sound insulation of windows with double glass units. Appl Acoust. 2015 May 1;92(Supplement C): p. 42–6.
6. Larbi W, Deü JF, Ohayon R. Vibroacoustic analysis of double-wall sandwich panels with viscoelastic core. Comput Struct. 2016 Oct;174: p. 92–103.
7. Sgard FC, Atalla N, Nicolas J. A numerical model for the low frequency diffuse field sound transmission loss of double-wall sound barriers with elastic porous linings. J Acoust Soc Am. 2000 Nov 21;108(6): p. 2865–72.
8. Guillaume P, Verboven P, Vanlanduit S, Van der Auweraer H, Peeters B. A Poly-Reference Implementation of the Least-Squares Complex Frequency-Domain Estimator. Proc IMAC 2003 Jan.
9. M El-Kafafy, B Peeters, T De Troyer, P Guillaume. Polymax Plus estimator: better estimation of the modal parameters and their confidence bounds. Proc ISMA2014 - USD2014; 15-17 September 2014; Leuven, Belgium 2014. p. 2469-84.
10. Standard ISO 10140 (2010) Acoustics - laboratory measurement of sound insulation of building elements: Part 1: Application rules for specific products; Part 2: Measurement of airborne sound insulation; Part 4: Measurement procedures and requirements; Part 5: Requirements for test facilities and equipment.